ELSEVIER

15 March 1996

Optics Communications 124 (1996) 519–528

OPTICS COMMUNICATIONS

Full length article

Diffraction of light by a corrugated magnetic grating: experimental results and calculation using a perturbation approximation to the Rayleigh method

D. van Labeke [a], A. Vial [a], V.A. Novosad [b,c], Y. Souche [b], M. Schlenker [b], A.D. Dos Santos [d]

[a] *Laboratoire d'Optique P.M. Duffieux, Université de Besançon, CNRS U.R.A. 214, U.F.R. Sciences, route de Gray, 25030 Besançon Cedex, France*

[b] *Laboratoire de Magnétisme Louis Néel du CNRS, Associé à l'Université Joseph Fourier, B.P. 166, 38042 Grenoble Cedex 9, France*

[c] *B. Verkin Institute for Low Temperature Physics and Engineering, Kharkov, Ukraine*

[d] *Instituto de Fisica, Univ. de Sao Paulo, Sao Paulo, Brazil*

Received 26 June 1995

Abstract

When visible light is diffracted by a relief grating covered with a ferromagnetic film, the intensity diffracted in all orders varies as magnetization is reversed. The relative variation in diffracted intensity is measured in the transverse, but generally non-specular, Kerr geometry (reflection case, magnetization perpendicular to diffraction plane). The effect is modelled using a perturbation approximation to the Rayleigh method. The theoretical results are in good agreement with experiment.

1. Introduction

The magneto-optical effects (Faraday effect in transmission, Kerr effects in reflection) have been known for a century. They were extensively used over the last three decades, both to measure magnetic properties and to image magnetic domains, and attracted considerable attention over the last 15 years in a successful effort to develop magneto-optical information storage technologies. In all cases, however, the Kerr effects were used in simple specular reflection.

When the magnetic material used has a periodic spatial structure, with a period on the order of 10^{-6} m, diffraction occurs for light, and the Kerr effects can be associated with *non-specular* geometries.

In this paper we discuss experiments performed on a one-dimensional magnetic grating in the geometry that, in specular reflection, corresponds to the transverse magneto-optical Kerr effect (TMOKE), and we give a theoretical analysis of their results.

In a previous set of experiments [1], we investigated the variation with applied magnetic field H_0 of $\delta I_p/I_p$, the relative variation in diffracted intensity for the diffracted beam of order p, when the magnetization $\boldsymbol{M}$ of a two-dimensional array of magnetic particles changes from saturation in one direction to saturation in the opposite direction, i.e. when moving along the hysteresis loop. We found that, under rather severe assumptions, we could associate the very different experimental diffraction loops with the mean distribution of magnetic domains. At that

SSDI 0030-4018(95)00598-6

time, we had to take the relative variations of diffracted intensity between the extreme situations at saturation, $\Delta I_p/I_p$, as phenomenological parameters.

Related experiments using the polar Kerr effect are conducted by Beauvillain et al. [2].

In the experimental part of the present paper, a preliminary version of which was given in Ref. [3], we focus on the simpler situation of a one-dimensional grating, and measure this small variation

$$\frac{\Delta I_p}{I_p} = \frac{I_p(M) - I_p(-M)}{I_p(M)}$$

of the intensity diffracted into order p between saturation in one direction, perpendicular to the scattering plane, and in the opposite direction.

We then present a first attempt to model this problem. Diffraction by a grating is an extensively studied subject in the case of isotropic material, but few papers address the anisotropic case. A bibliography and a description of the different methods can be found in a recent paper by Depine et al. [4]. A rigorous numerical method based on a coordinate transformation and which could be applied to any grating was proposed by Tayeb et al. [5,6]. Petit and Tayeb also mention a numerical investigation of diffraction by a corrugated magnetic surface which they performed in the polar Kerr geometry [7]. Glass [8] used a nonperturbative Rayleigh method to study nonreciprocal diffraction via grating coupling to surface magnetoplasmons in the millimetric range. By infinite order perturbation theory, Lu, Maradudin and Wallis [9] studied the enhanced backscattering of p waves by a random grating to which a constant magnetic field is applied.

In the experiments described below, the corrugation height is small compared to the wavelength. We therefore use for our calculation a first order perturbative approach based on the Rayleigh method. This approximation, that is restricted to linear terms in the surface profile function, was used in the past to study far-field diffraction by a random rough surface [10–13]. Recently it was also used in various models of near-field microscopy [14,15]. With such an approximation (perturbative Rayleigh method) we succeed to reproduce quite well the experimental measurements.

2. Sample, experimental setup, and results

Our diffraction grating consisted of a piece of a commercial Sony MiniDisk®, designed and marketed for magneto-optical audio recording, with nearly rectangular grooves 80 nm deep, and a period of $a = 1.6$ μm. The proprietary coatings, including the magnetically hard film with perpendicular anisotropy, were etched off with hydrofluoric acid. An amorphous soft magnetic film was sputtered on the bare polymer relief grating, using a magnetron triode device, operated at 10^{-2} torr, at room temperature, with an ionic current of 27 mA. Typical film thicknesses ranged from 40 to 150 nm. The sample shape was characterized using atomic force microscopy and a scanning electron microscope (SEM) and the composition verified using the X-ray emission analytic function of the SEM. The amorphous character of the film was checked using X-ray diffraction, the thickness was controlled during deposition by a quartz microbalance, and measured after growth with a Dektak 3030 surface profiling device. The magnetic properties were measured using a vibrating sample magnetometer, and the domains were observed with a low magnification Kerr effect optical microscope: in the absence of an applied field, the domains were several 10^{-1} mm wide, with magnetization approximately perpendicular to the grooves. In the transverse Kerr measurements, the magnetization was forced to rotate into the direction of the grooves.

A schematic diagram of the experiment is shown in Fig. 1. The measurements were based on an X-ray powder diffractometer, operated manually. The light source was a modulated laser diode, emitting at 0.67 μm wavelength. The detector was a photodiode, operated in the photoconductive mode. A polarizer was set across the incident beam, giving linear polarized light with electric field in the scattering plane. A lens concentrated the beam to an area about 0.1 mm in diameter on the grating. The sample was placed between the pole-pieces of a small electro-magnet, fed from a current-controlled DC bipolar amplifier driven by a low-frequency signal generator at a frequency between

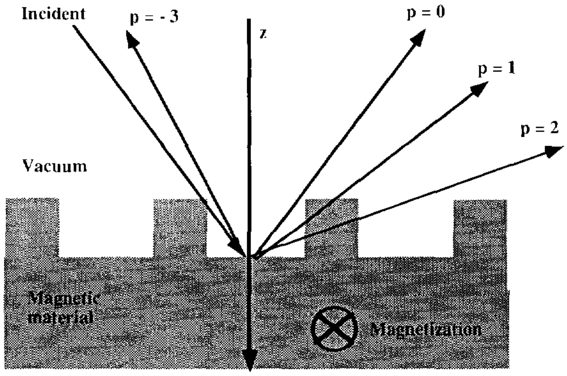

Fig. 1. Schematic diagram of the experimental setup and of the model used for the sample.

0.1 and 0.001 Hz, with amplitude sufficient to saturate the sample. The laser output was modulated with a frequency of about 1 kHz, and the output signal was fed to a lock-in amplifier connected to a microcomputer. The magnetic field at the sample position was measured using a Hall probe associated with a digital voltmeter.

Measurements of $\Delta I_p/I_p$ were made for all the diffracted orders, characterized by their index p. The direction i_p of the diffracted beam of order p is related to the angle of incidence by the grating relation $\sin(i_p) = \sin(i) + p\lambda/a$, where a is the grating period and λ the wavelength. Measurements are performed for various values of the angle of incidence i of the incident beam, obtained by turning the sample table of the X-ray diffractometer.

When studying the variations of $\Delta I_p/I_p$ as a function of the incidence angle i, Fig. 2 shows that some striking unity appears when the $\Delta I_p/I_p$ are plotted as a function of $(i_p + i)$, the angle between the diffracted and the incident beam. While the different orders show differences in their behavior, all $\Delta I_p/I_p$ go through zero for $i_p + i = 0$, i.e. for the situation when the diffracted beam is along the incident one (Littrow geometry).

The following theoretical study reproduces these phenomena.

3. Principle of the calculations

The geometry of our model is drawn on Fig. 1. The grating grooves are parallel to the y-axis and the z-axis points from vacuum into the magnetic material. The incident light comes from vacuum, the plane of incidence is the (x–z) plane which is perpendicular to the grooves. We only discuss the case of the transverse magneto-optical Kerr effect, hence the magnetization is along $\pm y$. We also suppose that we are in the saturation regime, i.e. the magnetic properties are constant along the grating profile. The dielectric tensor of the grating is then expressed as:

$$\epsilon = \begin{bmatrix} \epsilon_1 & 0 & -\mathrm{i}\eta \\ 0 & \epsilon_1 & 0 \\ +\mathrm{i}\eta & 0 & \epsilon_1 \end{bmatrix}, \tag{1}$$

where ϵ_1 is the usual isotropic dielectric constant and η the small magneto-optical term. Reversing the direction of magnetization $\boldsymbol{M}$ corresponds to changing η into $-\eta$. We assume that the material is, apart from the magneto-optical contribution, isotropic.

In order to simplify the discussion, we suppose that the magnetic layer is thick enough to mask the influence of the under-layer. The grating is thus described by the equation of the interface which can be expressed as a Fourier series:

$$P(x) = \sum_{n=-\infty}^{\infty} P(n) \exp(2\mathrm{i}\pi x n/a) . \tag{2}$$

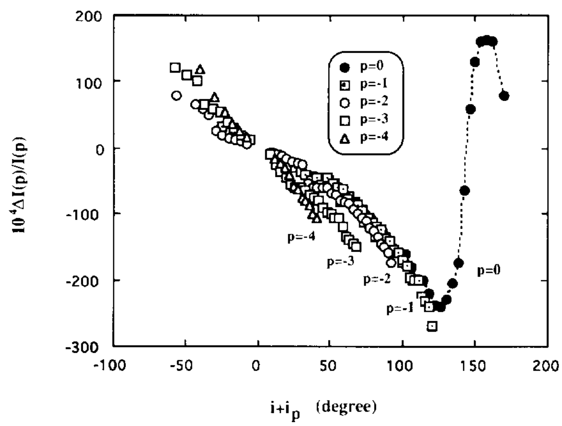

Fig. 2. Measured relative variation of diffraction intensity associated with reversal of magnetization, $\Delta I_p/I_p$, for the various diffraction orders p. The curves are plotted versus $i+i_p$, where i is the angle of incidence and i_p is the angle of the diffracted beam p with respect to the surface normal.

We note λ the incident wavelength in vacuum. In the following, all the wave vector components, in units of $2\pi/\lambda$, are denoted as $\{\alpha, \beta, \gamma\}$ with subscripts and superscripts to distinguish the various vectors. Since we only consider diffraction in the principal plane, all the wave vectors have $\beta=0$.

The incident field is expressed as:

$$\boldsymbol{E}^{\text{inc}}(x, z) = \boldsymbol{E}^{\text{inc}} \exp(\mathrm{i}\boldsymbol{K}_{\text{inc}} \cdot \boldsymbol{r}) , \tag{3}$$

where $\boldsymbol{K}_{\text{inc}}$ is the incident wave vector:

$$\boldsymbol{K}_{\text{inc}} = \frac{2\pi}{\lambda} \{\alpha_{\text{inc}}, 0, \gamma_{\text{inc}}\} = \frac{2\pi}{\lambda} \{\sin(i), 0, \cos(i)\} . \tag{4}$$

The amplitude of the incident field contains, in the general case, both a Transverse Electric (TE) and a Transverse Magnetic (TM) component. We note A_1^{inc} and A_2^{inc} the corresponding amplitudes, hence we have the relation:

$$\boldsymbol{E}^{\text{inc}} = \{\gamma_{\text{inc}} A_2^{\text{inc}}, A_1^{\text{inc}}, -\alpha_{\text{inc}} A_2^{\text{inc}}\} . \tag{5}$$

In vacuum and in the magnetic material, the diffracted electric fields can be expressed as Rayleigh expansions:

$$\boldsymbol{E}^0(x, z) = \sum_{p=-\infty}^{+\infty} \sum_{\sigma=1,2} A_\sigma^0 \boldsymbol{E}_\sigma^0(p) \exp\{2\mathrm{i}\pi[\alpha(p)x - \gamma(p)z]/\lambda\} \qquad z<P(x) , \tag{6a}$$

$$\boldsymbol{E}^1(x, z) = \sum_{p=-\infty}^{+\infty} \sum_{\sigma=1,2} A_\sigma^1 \boldsymbol{E}_\sigma^1(p) \exp\{2\mathrm{i}\pi[\alpha(p)x + \gamma_\sigma^1(p)z]/\lambda\} \qquad z>P(x) . \tag{6b}$$

In Eqs. (6), the subscript σ corresponds to the different modes ($\sigma=1$ for TE, 2 for TM) and the index p to the various diffracted orders ($p=-\infty, +\infty$). In each term the superscript labels the medium: 0 for vacuum, 1 for the magnetic material.

The x components of all the diffracted wave vectors verify the grating equation:

$$\alpha(p) = \sin(i_p) = \alpha_{\text{inc}} + p\lambda/a . \tag{7}$$

The z component of the wave vectors are obtained via the dispersion relation. In vacuum we obtain:

$$\gamma(p) = \sqrt{1-\alpha(p)^2} . \tag{8}$$

In vacuum, the Rayleigh expansion is thus made up of both propagating and evanescent plane waves. $\gamma(p)$ is real for propagating homogeneous waves, and purely imaginary for the evanescent waves.

In vacuum, the modes are the classical TE ($\sigma=1$) and TM ones ($\sigma=2$):

$$E_1^0(p)=\{0,1,0\} \qquad E_2^0(p)=\{\gamma(p),0,-\alpha(p)\}. \tag{9}$$

In the magnetic material, in the case of the transverse Kerr effect the modes can be calculated, for instance using formalism and equations of Ref. [16].

$\sigma=1$ corresponds to a TE mode which does not reflect any magnetic property:

$$\gamma_1^1(p)=\sqrt{\epsilon_1-\alpha(p)^2} \quad \text{and} \quad E_1^1(p)=\{0,1,0\}. \tag{10}$$

$\sigma=2$ corresponds to a TM mode but the magneto-optical constant is contained in the wave vector and in the mode expression:

$$\gamma_2^1(p)=\sqrt{\epsilon_1-\alpha(p)^2-\eta^2/\epsilon_1}, \qquad E_2^1(p)=\left\{1,0,\frac{\epsilon_1-[\gamma_2^1(p)]^2}{\mathrm{i}\eta-\alpha(p)\gamma_2^1(p)}\right\}. \tag{11}$$

The calculation of the diffracted amplitude A_σ^i ($i=0,1$; $\sigma=1,2$) is a very difficult task for a general grating. However, the gratings used in the present experiments have a height small compared with the wavelength. For such a shallow grating the Rayleigh hypothesis leads to good results. It assumes that the expansions (6) remain valid inside the grooves and can be used for matching the fields at the boundary.

At the grating surface the tangential components of the electric and magnetic fields must be continuous:

$$\begin{aligned} &\boldsymbol{n}\wedge[\boldsymbol{E}^{\mathrm{inc}}(x,z)+\boldsymbol{E}^0(x,z)]=\boldsymbol{n}\wedge\boldsymbol{E}^1(x,z) \text{ for } z=P(x),\\ &\boldsymbol{n}\wedge[\boldsymbol{H}^{\mathrm{inc}}(x,z)+\boldsymbol{H}^0(x,z)]=\boldsymbol{n}\wedge\boldsymbol{H}^1(x,z) \text{ for } z=P(x), \end{aligned} \tag{12}$$

where $\boldsymbol{n}$ is the unit vector normal to the grating surface. The magnetic field is easily calculated by applying Maxwell's equations to the electric fields (6).

Moreover, as the grating corrugation has a height small compared to the wavelength, the exponentials occurring in the boundary conditions can be expanded into a series, for instance:

$$\exp[\mathrm{i}\gamma_\sigma^1 P(x)]\approx 1+\mathrm{i}\gamma_\sigma^1 P(x)+\dots. \tag{13}$$

With (13) restricted to the linear terms the field amplitudes can be split into two terms:

$$A_\sigma^i(p)=F_\sigma^i(p)\,\delta_{p0}+D_\sigma^i(p\neq 0) \qquad (\sigma=1,2;\ i=0,1). \tag{14}$$

The first term of each Eq. (14) corresponds respectively to the fields reflected (F_σ^0) and transmitted (F_σ^1) by a flat interface without roughness. This corresponds, in the present approximation, to the zeroth order of diffraction. The second terms are the actual diffracted fields in vacuum (D_σ^0) and in the grating (D_σ^1). When these equations are injected into the boundary conditions (12), we obtain a set of equations which can be solved by iteration.

We first get relations that connect the reflected and transmitted fields to the incident field:

$$\mathbf{M}^1(0)\times\begin{bmatrix}\mathbf{F}_1^1\\0\\\mathbf{F}_2^1\\0\end{bmatrix}=\mathbf{M}^0(0)\times\begin{bmatrix}\mathbf{A}_1^{\mathrm{inc}}\\\mathbf{F}_1^0\\\mathbf{A}_1^{\mathrm{inc}}\\\mathbf{F}_2^0\end{bmatrix}, \tag{15}$$

where $\mathbf{M}^0(p)$ and $\mathbf{M}^1(p)$ are 4×4 matrices:

$$\mathbf{M}^0(p)=\begin{bmatrix} 1 & 1 & 0 & 0 \\ -\gamma(p) & \gamma(p) & 0 & 0 \\ 0 & 0 & \gamma(p) & -\gamma(p) \\ 0 & 0 & 1 & 1 \end{bmatrix}, \tag{16a}$$

$$\mathbf{M}^1(p)=\begin{pmatrix} 1 & 1 & 0 & 0 \\ -\gamma_1^1(p) & \gamma_1^1(p) & 0 & 0 \\ 0 & 0 & 1 & 1 \\ 0 & 0 & \gamma_2^1(p)-\alpha(p)\dfrac{\epsilon_1-[\gamma_2^1(p)]^2}{\mathrm{i}\eta-\alpha(p)\gamma_2^1(p)} & -\gamma_2^1(p)-\alpha(p)\dfrac{\epsilon_1-[\gamma_2^1(p)]^2}{\mathrm{i}\eta+\alpha(p)\gamma_2^1(p)} \end{pmatrix}. \tag{16b}$$

Matrices (16) are block diagonal, which corresponds to the familiar result that in the TMOKE geometry the TE and TM polarizations are not coupled [17,18]. By using Eqs. (15)–(16) the reflected amplitudes can be expressed as a function of the incident ones:

$$F_1^0=\frac{\gamma(0)-\gamma_1^1(0)}{\gamma(0)+\gamma_1^1(0)}A_1^{\mathrm{inc}}, \tag{17a}$$

$$F_2^0=\frac{\alpha[\epsilon_1\gamma(0)-\gamma_2^1(0)]-\mathrm{i}\eta[\gamma(0)\gamma_2^1(0)-1]}{\alpha[\epsilon_1\gamma(0)+\gamma_2^1(0)]-\mathrm{i}\eta[\gamma(0)\gamma_2^1(0)+1]}A_2^{\mathrm{inc}}. \tag{17b}$$

The diffracted amplitudes $D_\sigma^i(p)$ $(p\neq 0)$ also verify a linear system, but with a more complicated structure:

$$\mathbf{M}^1(p)\times\begin{bmatrix}\mathbf{D}_1^1(p)\\ 0\\ \mathbf{D}_2^1(p)\\ 0\end{bmatrix}=\mathbf{M}^0(p)\times\begin{bmatrix}0\\ \mathbf{D}_1^0(p)\\ 0\\ \mathbf{D}_2^0(p)\end{bmatrix}+\frac{2\mathrm{i}\pi P(p)}{\lambda}\left(\mathbf{N}^1\times\begin{bmatrix}\mathbf{F}_1^1\\ 0\\ \mathbf{F}_2^1\\ 0\end{bmatrix}+\mathbf{N}^0\times\begin{bmatrix}\mathbf{A}_1^{\mathrm{inc}}\\ \mathbf{F}_1^0\\ \mathbf{A}_2^{\mathrm{inc}}\\ \mathbf{F}_2^0\end{bmatrix}\right), \tag{18}$$

$$\mathbf{N}^0=\begin{bmatrix} 0 & 0 & 0 & 0 \\ -[\gamma(0)]^2 & -[\gamma(0)]^2 & 0 & 0 \\ 0 & 0 & -\alpha(0)p\lambda/a+[\gamma(0)]^2 & -\alpha(0)p\lambda/a+[\gamma(0)]^2 \\ 0 & 0 & \gamma(0) & -\gamma(0) \end{bmatrix}, \tag{19}$$

$$\mathbf{N}^1=\begin{pmatrix} 0 & 0 & 0 & 0 \\ \gamma_1^1(0)]^2 & [\gamma_1^1(0)]^2 & 0 & 0 \\ 0 & 0 & -\gamma_2^1(0)-p\dfrac{\lambda}{a}\dfrac{\epsilon_1-[\gamma_2^1(0)]^2}{\mathrm{i}\eta-\alpha(0)\gamma_2^1(0)} & +\gamma_2^1(0)-p\dfrac{\lambda}{a}\dfrac{\epsilon_1-[\gamma_2^1(0)]^2}{\mathrm{i}\eta+\alpha(0)\gamma_2^1(0)} \\ 0 & 0 & -\gamma_2^1(0)+\alpha(0)\gamma_2^1(0)\dfrac{\epsilon_1-[\gamma_2^1(0)]^2}{\mathrm{i}\eta-\alpha(0)\gamma_2^1(0)} & \gamma_2^1(0)-\alpha(0)\gamma_2^1(0)\dfrac{\epsilon_1-[\gamma_2^1(0)]^2}{\mathrm{i}\eta+\alpha(0)\gamma_2^1(0)} \end{pmatrix}. \tag{20}$$

In Eq. (18) the diffracted amplitudes $D^1_\sigma(p)$ in the grating are linearly related to the diffracted amplitudes in vacuum $D^0_\sigma(p)$ by the same matrices as in Eq. (15), but calculated for the order p of diffraction. Eq. (18) also contains terms proportional to the Fourier coefficient $P(n)$ of the grating profile multiplied by coefficients that relate the amplitudes incident on, and reflected or transmitted by a flat interface.

Using Eqs. (15)–(20), the calculation of the diffracted amplitudes in vacuum $D^0_\sigma(p)$ can be completed. The analytical expressions thus obtained are rather long and cannot be reproduced in this paper. We can notice that matrices $\mathbf{N}^1$, $\mathbf{N}^0$ also have a block diagonal structure, like $\mathbf{M}^0(p)$ and $\mathbf{M}^1(p)$. The results obtained for a flat interface thus remain valid for a grating illuminated in the principal plane: in TMOKE diffraction geometry, the TE and TM modes are not coupled, there is neither depolarization nor rotation of the polarization, and a magneto-optical effect can only be observed in TM polarization. This property is also underlined in Ref. [9] in the case of a random 1D surface.

4. Results of the calculations

In order to compare these theoretical results with the experiments, we take the case of amorphous Fe_3Si. The wavelength used is $\lambda = 670$ nm. The optical constants were derived from measurements on flat surfaces. We study the experimentally observed variations in the case of specular reflection of $\Delta I/I$, versus the angle of incidence i. Because within our approximation the reflected order $p=0$ corresponds to the specular reflection, the experimental results can be fitted by using Eqs. (15)–(17) or by similar results described in Ref. [19]. The resulting values of the optical constant are $\epsilon_1 = 5.3 + 6.5\mathrm{i}$ and $\eta = -0.112 - 0.0003\mathrm{i}$. The curve of variations is shown in Fig. 3.

Our formalism is then applied for calculating the magneto-optical effect from a grating. The grating has a rectangular structure with period $a = 1600$ nm, width $b = 600$ nm and height $c = 80$ nm. When changing the angle of incidence three or four diffracted propagating modes can be produced. For each mode we can calculate the intensity:

$$I(p) = \frac{\gamma(p)}{\gamma(0)} \frac{|D^0_\sigma(p)|^2}{2\mu_0 c} \tag{21}$$

and thus deduce the $\Delta I_p/I_p$ corresponding to the reversal of magnetization $\boldsymbol{M}$.

Fig. 4 shows the calculated results for various harmonics, versus the deviation angle between the incident and the diffracted beam $(i + i_p)$, where i_p is the angle of the diffracted beam of order p. They can be compared with the

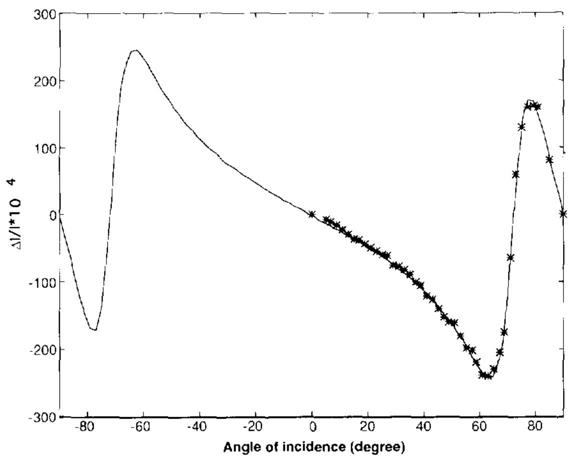

Fig. 3. Calculated relative variation of the intensity when magnetization is reversed, $\Delta I/I$, for specular reflection, versus the angle of incidence. The experimental points are used to determine the optical constants: $\epsilon_1 = 5.3 + 6.5\mathrm{i}$ and $\eta = -0.112 - 0.0003\mathrm{i}$.

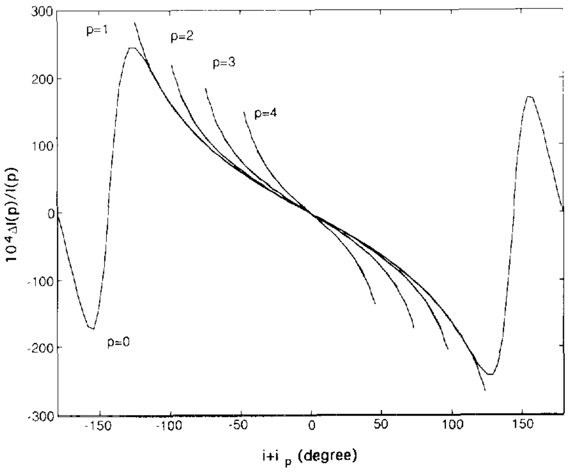

Fig. 4. Calculated values of $\Delta I_p/I_p$ for the various orders p, assuming values of the optical constants $\epsilon_1 = 5.3 + 6.5i$ and $\eta = -0.112 - 0.0003i$. All the curves are plotted versus the angle of deviation $(i + i_p)$. Curves with opposite values of p coincide.

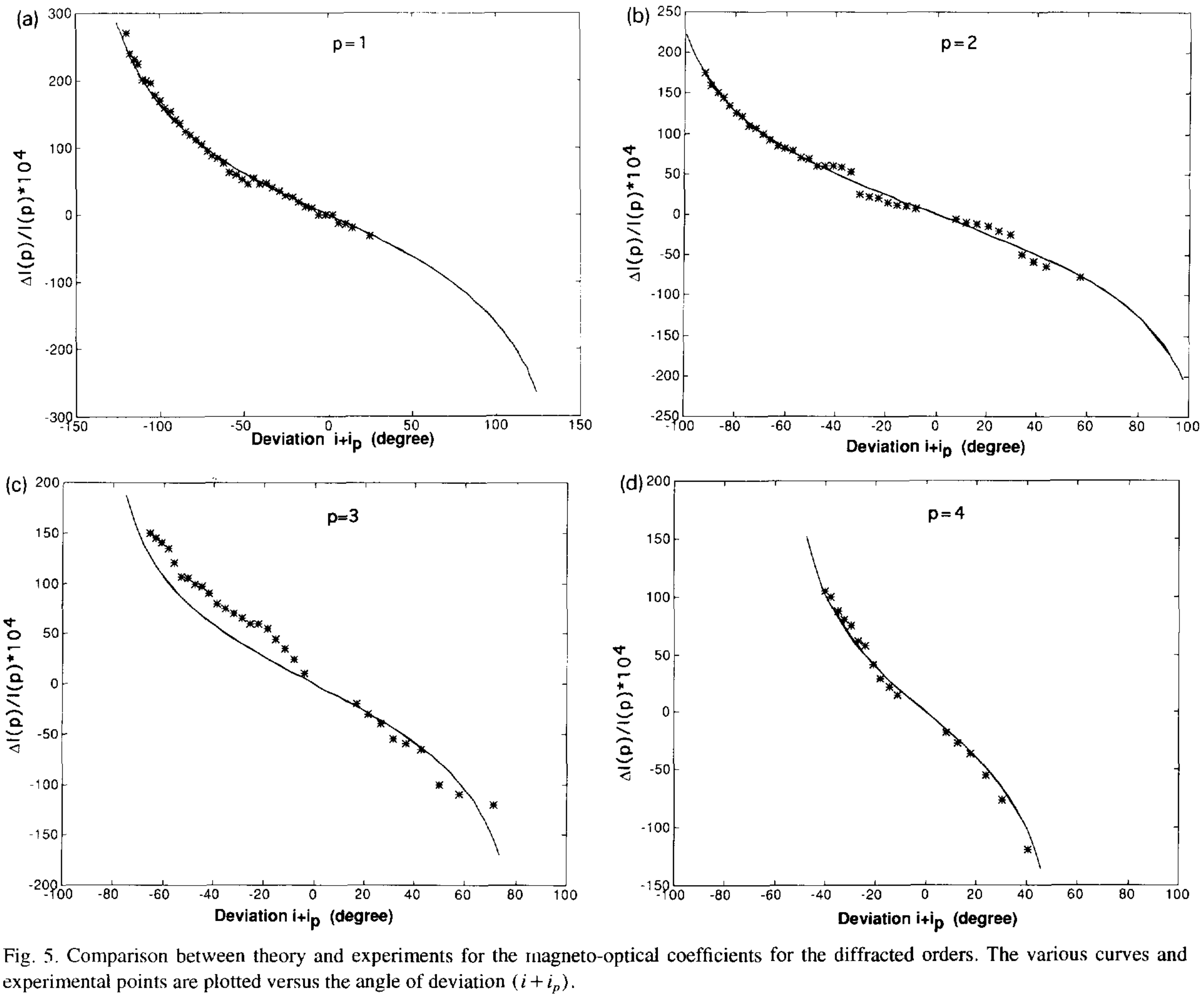

Fig. 5. Comparison between theory and experiments for the magneto-optical coefficients for the diffracted orders. The various curves and experimental points are plotted versus the angle of deviation $(i + i_p)$.

experimental results of Fig. 2. Let us notice that all the curves have a center of symmetry: the point $(i = -i_p, 0)$. Moreover the curves corresponding to opposite values of p are the same.

The calculations reproduce the interesting result described in the experimental part: all the curves have a common intersection point. The TMOKE coefficients change sign when the angle of incidence is changed. The zero point of all these curves is obtained for the angle satisfying $i = -i_p$. Moreover the experimental values are in good agreement with the calculations.

The comparison between experimentals results and theoretical calculations is presented in Figs. 5. The theoretical curves are deduced from equations of Section 2. The optical constants are those obtained from the specular reflection (Fig. 2). We can conclude a good agreement between measurements and theory. The residual discrepancy between points and curves could be explained by experimental uncertainties but also to the fact that the exact sample profile is unknown.

5. Discussion

We have, both experimentally and, using the Rayleigh expansion and a perturbation method, theoretically investigated the diffraction of a plane wave by a relief magneto-optical grating in the transverse Kerr geometry. The calculations agree quite well with the experimental results both qualitatively and quantitatively.

When experimental parameters are precisely determined (the exact shape of the grating grooves is still rather unknown), we plan to refine the theoretical calculation. The perturbation method could be replaced by the exact Rayleigh method [4,8,9] or a more rigorous calculation [e.g. 5–7]. However, these methods are more complicated and involve larger computations.

In the case of shallow grating, the perturbative method leads to a correct description of the phenomena and of the experimental results. So this method could be applied for other magneto-optical effects (longitudinal or polar Kerr effect), calculations are in in progress. Far-field diffraction is a good way for studying magneto-optical samples and the theoretical method described in this paper is a simple tool to determine the physical parameters from experiments.

The authors would like to thank A. Liénard for the SEM measurements, C. Hordequin and C. Bordel for help in sputtering, and H. Joisten, of LETI, for the AFM tests.

References

[1] O. Geoffroy, D. Givord, Y. Otani, B. Pannetier, A.D. Santos, M. Schlenker and Y. Souche, J. Magn. Magn. Mater. 121 (1993) 516.
[2] N. Bardou, B. Bartenlian, F. Rousseau, D. Decanini, F. Carcenac, C. Chappert, P. Veillet, P. Beauvillain, R. Mégy, Y. Susuki and J. Ferré, Light diffraction effects in the magnetooptical properties of 2D arrays of magnetic dots of Au/Co/Au(111) films with perpendicular magnetic anisotropy, Journal of Magnetism and Magnetic Materials, to be published.
[3] Y. Souche, M. Schlenker and A.D. Dos Santos, J. Magn. Magn. Mater. 140–144 (1995) 2179.
[4] R.A. Depine and M.L. Gigli, J. Mod. Optics. 41 (1994) 695.
[5] G. Tayeb, M. Cadilhac and R. Petit, C.R. Acad. Sci., Paris 307 (1988) 711.
[6] G. Tayeb, C.R. Acad. Sci., Paris 307, Serie II (1988) 1501.
[7] R. Petit and G. Tayeb, Proc. SPIE 815 (1987) 11.
[8] N.E. Glass, Phys. Rev. B 41 (1990) 7165.
[9] J.Q. Lu, A.A. Maradudin and R.F. Wallis, Waves Random Media 1 (1991) 309.
[10] A. Maradudin and D. Mills, Phys. Rev. B 11 (1990) 1392.
[11] F. Toigo, A. Marvin, V. Celli and N.R. Hill, Phys. Rev. B 13 (1977) 5618.
[12] G.S. Agarwal, Phys. Rev. B 15 (1977) 2371.
[13] J.J. Greffet, Phys. Rev. B 37 (1988) 6436.
[14] D. Van Labeke and D. Barchiesi, J. Opt. Soc. Am. A 9 (1992) 732.

[15] D. Van Labeke, F. Baida, D. Barchiesi and D. Courjon, Opt. Comm. 114 (1995) 470.
[16] H.C. Chen, Theory of Electromagnetic Waves (MacGraw–Hill, New York, 1995).
[17] G. Metzger, P. Pluvinage and R. Torguet, Ann. Phys. (Paris) 10 (1965) 5.
[18] H.T. Minden, Appl. Optics 29 (1990) 3955.
[19] D.H. Martin, K.F. Neal and T.J. Dean, Proc. Phys. Soc. 86 (1965) 605.